STREAM

IST-1999-10341

STREAM CONSORTIUM:
CNR-LAMEL / ST Microelectronics / ISEN / SOFT IMAGING SYSTEM / University of Sheffield / IMEC / CNR-IESS / University of Perugia

DELIVERABLE D10

Workpackage WP3

Lead participant: CNR-LAMEL

Investigation of different zone axes for TEM/CBED analysis

Main Author	A.Armigliato, CNR-LAMEL		
Contributing authors	R.Balboni, S.Frabboni, CNR-LAMEL; G.Pavia (ST); T.Schilling (SIS), A.G.Cullis, A.Benedetti (USFD)		
Date:	31 01 2001	***Doc.No:***	IST10341-LA-RP006
Keywords:	Strain, shallow trenches, electron microscopy, convergent beam electron diffraction, zone axis, energy filtering		

Distribution list	**Project Officer:** B.Netange (3 copies) **All Partners:** G.P.Carnevale ST Microelectronics V. Senez ISEN T. Schilling Soft Imaging System A.G.Cullis USFD (University of Sheffield) I. De Wolf IMEC S. Lagomarsino CNR-IESS G. Carlotti UniPg (University of Perugia)

Table of contents

Abstract

The need of exploring the feasibility of performing TEM/CBED work by using crystallographic projections other than the <130> has been prompted by the significant, unwanted projection effects induced by the required tilting of 26.5° along the direction normal to the wafer axis. It is worth remembering that to analyse the STI structures of 1st measurement campaign, we have worked at 100 kV in the <130> projection.

To this end, other crystallographic projections are considered, with the aim of minimising the angle of tilt of the investigated cross sectioned STI structures. It has been tested in detail the projection <230>, which corresponds to a tilt angle of 11.3°, i.e. much smaller than for the <130>. In addition to varying the tilt angle, it has been increased the acceleration voltage of the electron beam of the TEM from 100 kV to 200 kV, with a positive effect on the gun brightness (which reduces the acquisition time of a CBED pattern) and on the maximum thickness of the local region of the STI that can be analysed. The results of application of this procedure to the samples of the 1st measurement campaign are reported in this Deliverable; a comparison with the corresponding results of the first campaign, as well as with the IMPACT simulation, will also be made.

1. Introduction

The strain analysis carried out so far by TEM/CBED on the samples of the 1st Measurement Campaign (see Deliverables D1 and D5) are based on the acquisition of diffraction patterns taken at an electron acceleration voltage of 100 kV and with the samples tilted to the <130> crystallographic projection. The reason of this choice lies in the large experience gained in the past decade by the CNR-LAMEL Institute in the determination by TEM/CBED of strain tensors in silicon and silicon-germanium alloys, where the choice of these experimental parameters proved to be appropriate. In fact, the results obtained in silicon-germanium films of different composition were in agreement with those deduced from other techniques (double-crystal X-ray diffraction, ion beam channeling).

However, the use of the above conditions presents the following two main limitations:

1. The acceleration voltage of 100 kV is available in all the electron microscopes operating in the field of materials science, however it is not the most frequently used in the instruments with the maximum voltage of 200 or 300 kV, which are presently of most widespread use, particularly in the field of microelectronics. This depends on the rather complex procedures of alignment of the TEM electron optics, including the energy filter (if present). Moreover, the brightness of the electron gun increases with the electron beam, so at 200 kV the beam intensity is higher, and in turn the time of acquisition of a CBED pattern is shorter, than at 100 kV.
2. Still more important in the case of the investigation of deep sub-micron electronic devices, the angle of specimen tilt required to move from the horizontal <110> orientation to the <130> crystallographic projection is 26.5°. This results in a significant projection effect, which reduces the width of the active region of the device (e.g. an STI structure) that can be effectively analysed by the TEM/CBED technique; this is also related to the local thickness of the TEM cross section, suitable for the acquisition of patterns of sufficient quality, which for silicon is in the range of 200 nm. Therefore, with the scaling down of the size of the test patterns to be used during the STREAM activity and beyond it, a reduction in the tilt angel of the specimen is strongly advisable.

For these reasons, the possibility of using crystallographic projections other than the <130> has been explored and the results will be reported in this Deliverable. An acceleration voltage of 200 kV has been chosen for the new experiments, both for the reasons explained above and because the TEMs available in the laboratories of the partners ST and USFD are 200 kV microscopes (the one at CNR-LAMEL is a 300 kV one, but it can equally well work at 200 kV).

2. Zone axes for TEM/CBED analysis of silicon, more favourable than <130>

As mentioned in the Introduction, the need for tilt angles of the TEM cross section lower than the <130> so far employed, is becoming more and more stringent with the scaling down of the electronic device, due to the large, unwanted projection Of course, as the CBED pattern must contain an adequate number of HOLZ lines and the pattern must be simulated by the software which yields the strain tensor, only clearly and easily identifiable crystallographic projections (zone axes) are to be selected. Therefore only a discrete number of tilt angles between the <130> and the <110> area suitable for the CBED analysis. Its is worthwhile noting that the <110> projection (tilt angle 0°, i.e. specimen kept horizontal), cannot be used, due to the excessive number of HOLZ lines present in the corresponding CBED pattern and the dynamical character of most of them. As detailed in the Deliverable D2, the simulation of the HOLZ line pattern can be best performed in the kinematical approximation; in fact, the dynamical simulation is not impossible, but by far more complicated and time consuming.

In the following, it will be reported for comparison the arrangements of the HOLZ lines, as take place in the CBED patterns taken in 4 different zone axes, including the <130> one. The Miller indices, as well as the tilt angles required to get to these axes from the <110> horizontal projections, are reported in Table 1.

Table 1. Miller indices of a few zone axes in cubic crystals (e.g. silicon) and corresponding tilt angles from the horizontal <110> projection.

Miller indices	Tilt angle (deg.)
<130>	26.5
<120>	18.4
<230>	11.3
<560>	5.2
<110>	0

2.1 Simulated and corresponding experimental CBED patterns at 100 kV

The first step is to predict how it will change the disposition and the number of the HOLZ lines, when the sample will be tilted into the different zone axes. Initially, it will be chosen the acceleration voltage of 100 kV, which is the one employed in all the previous experiments performed at CNR-LAMEL, including the 1st measurement campaign, and also the one used by the other partners (USFD and ST).

The simulation is useful to understand if a given projection can be actually employed in a real TEM/CBED experiment. To this end, a computer programme written by J.P.Morniroli [1] has been used. This programme adopts a kinematical approach and displays the HOLZ lines irrespective of their belonging to the different Laue zones, down to a chosen minimum value of the corresponding interplanar spacing. Moreover, it gives no information on the intensity of the HOLZ lines. In Figure 2.1 to Figure 2.5 are shown the simulated CBED patterns at 100 kV for the 5 zone axes reported in Table 1, together with the corresponding experimental ones.

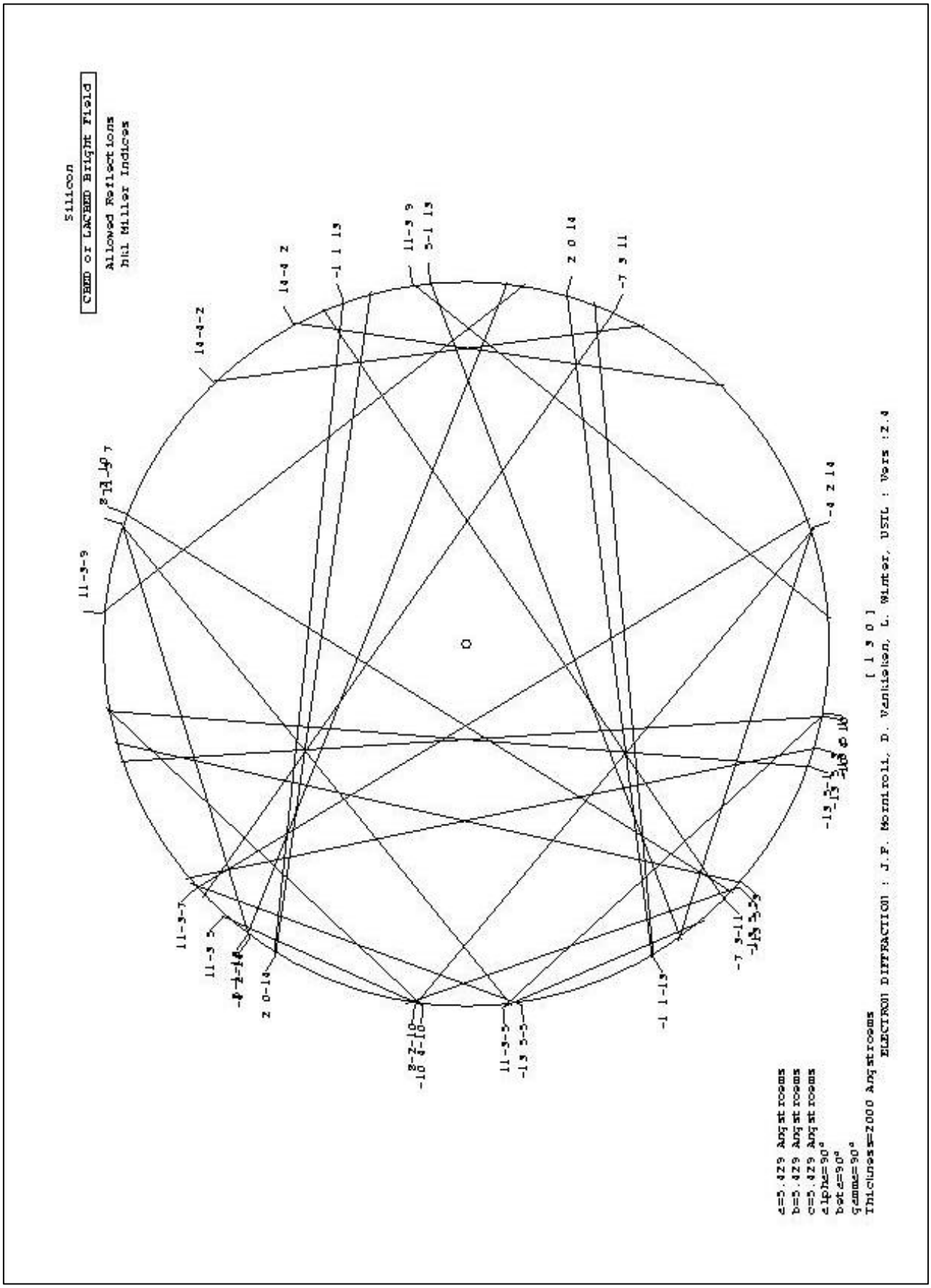

Figure 2.1. a) Simulated CBED pattern taken in the <130> zone axis at 100 kV. The tilt axis, parallel to the <100> growth direction, is horizontal. Tilt angle off the <110> orientation: 26.5°.Note the similarities with the experimental patterns reported in Deliverables D2 and D5.

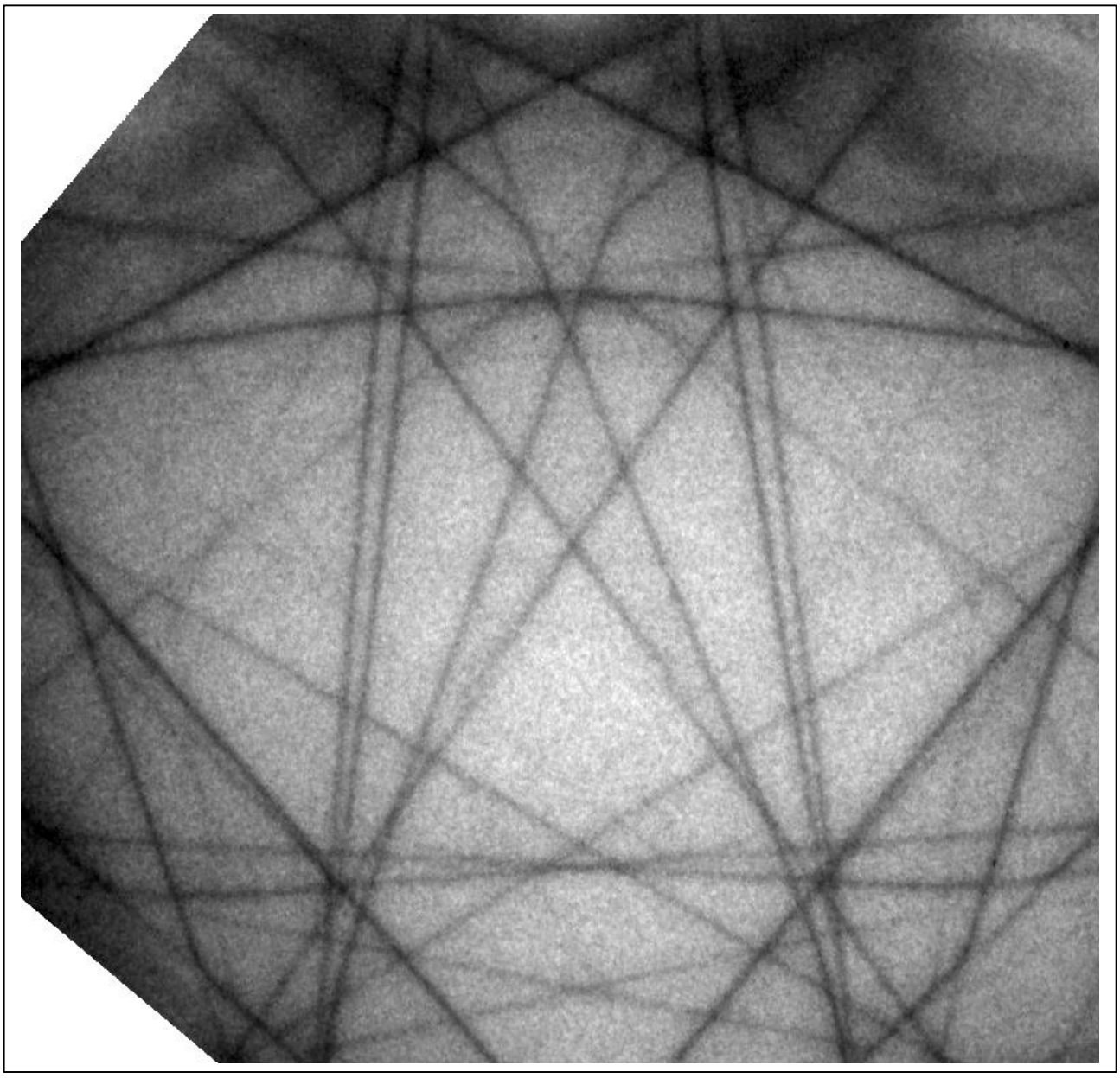

b) Corresponding experimental CBED pattern taken in the <130> zone axis at 100 kV

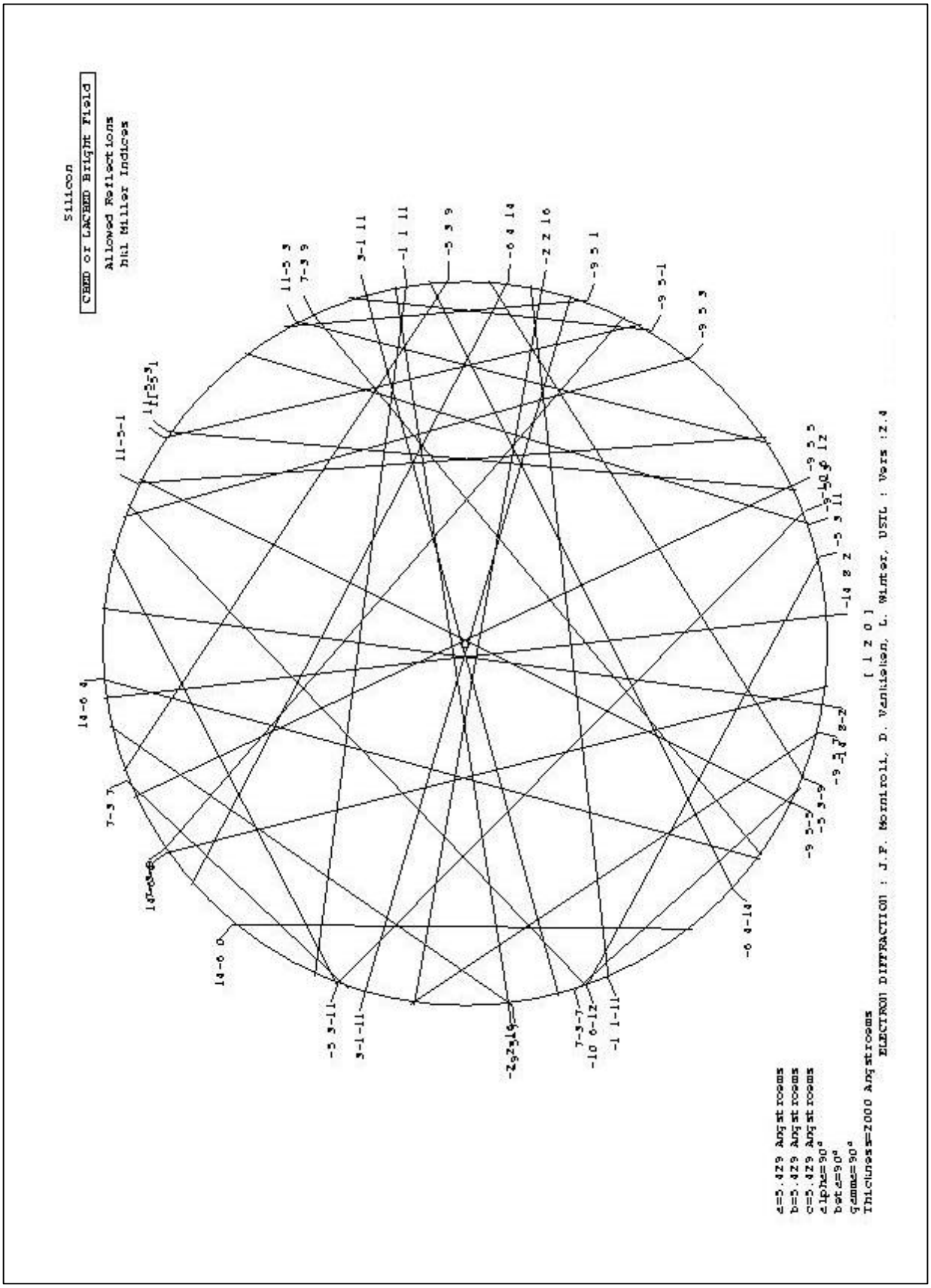

Figure 2.2. a) Simulated CBED pattern taken in the <120> zone axis at 100 kV. The tilt axis, parallel to the <100> growth direction, is horizontal. Tilt angle off the <110> orientation: 18.4°

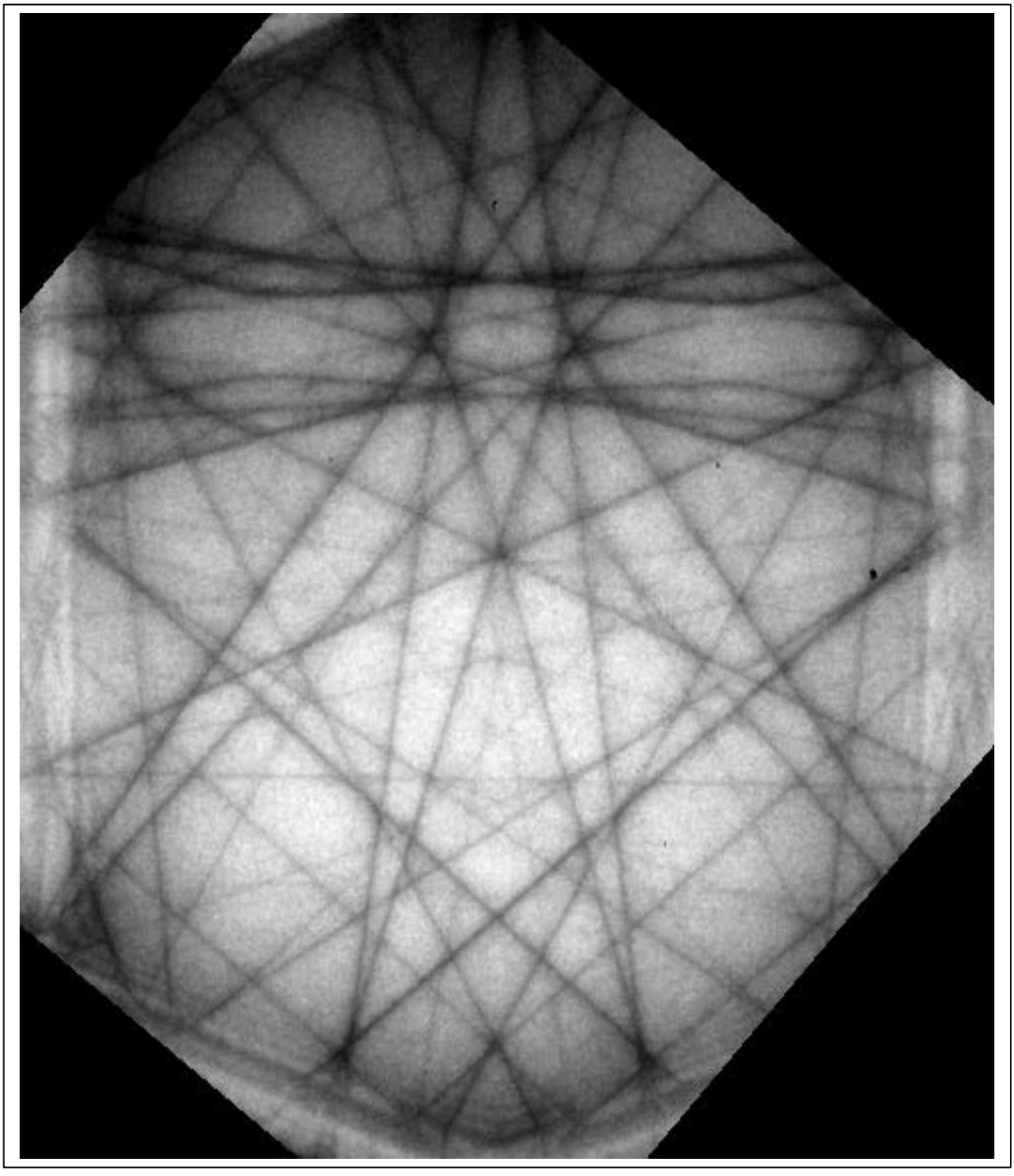

b) Corresponding experimental CBED pattern taken in the <120> zone axis at 100 kV

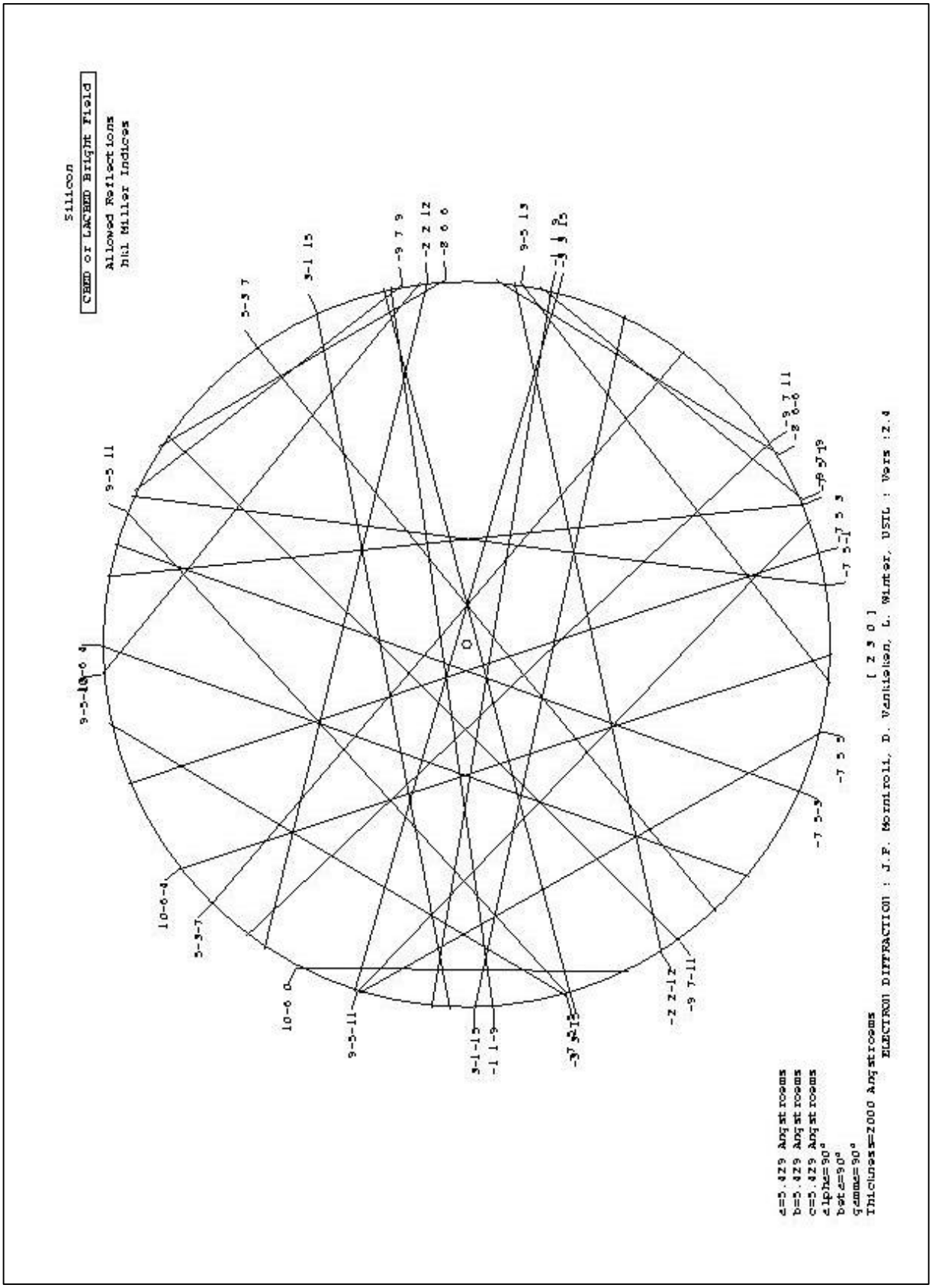

Figure 2.3. a) Simulated CBED pattern taken in the <230> zone axis at 100 kV. The tilt axis, parallel to the <100> growth direction, is horizontal. Tilt angle off the <110> orientation: 11.3°

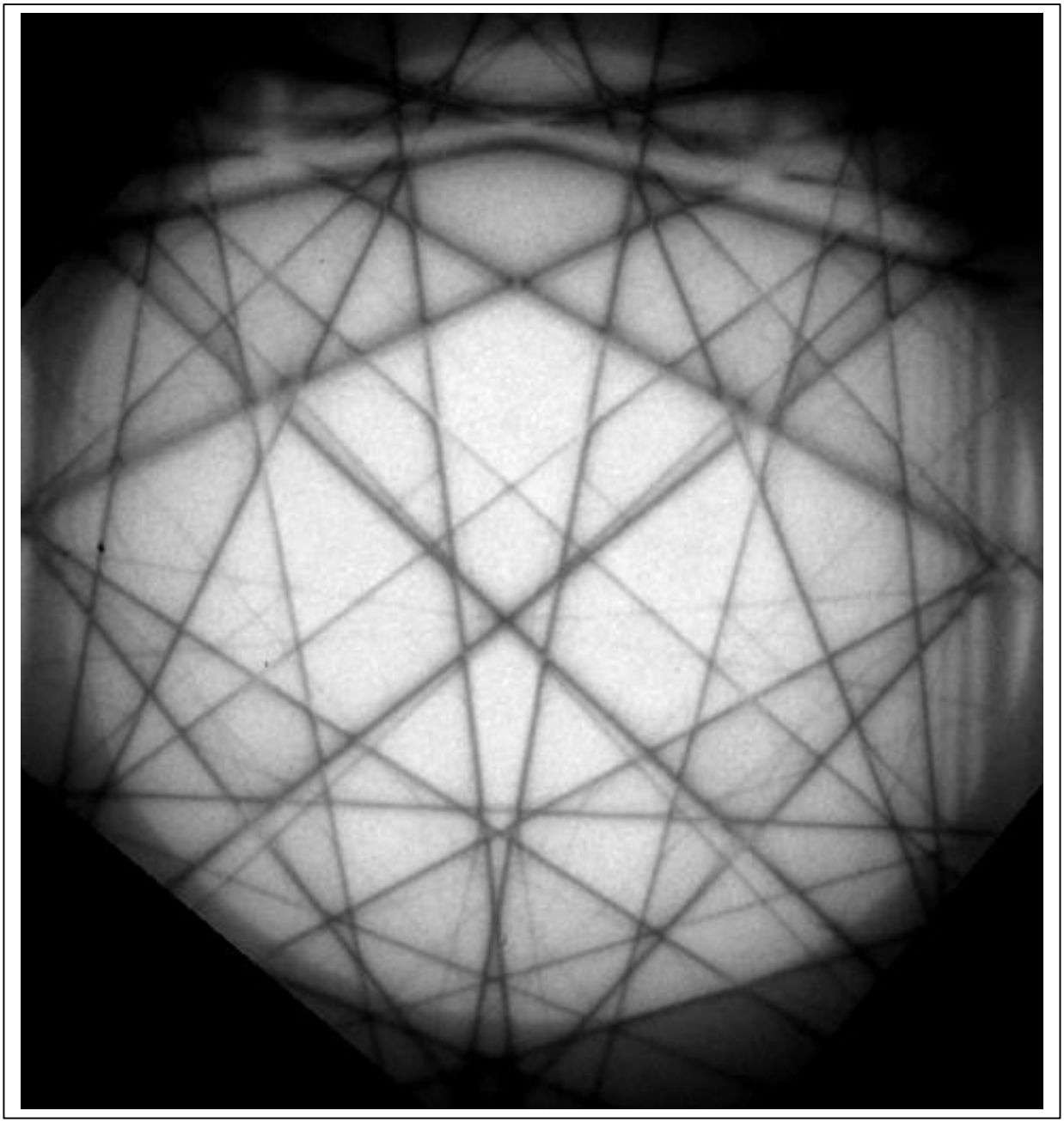

b) Corresponding experimental CBED pattern taken in the <230> zone axis at 100 kV

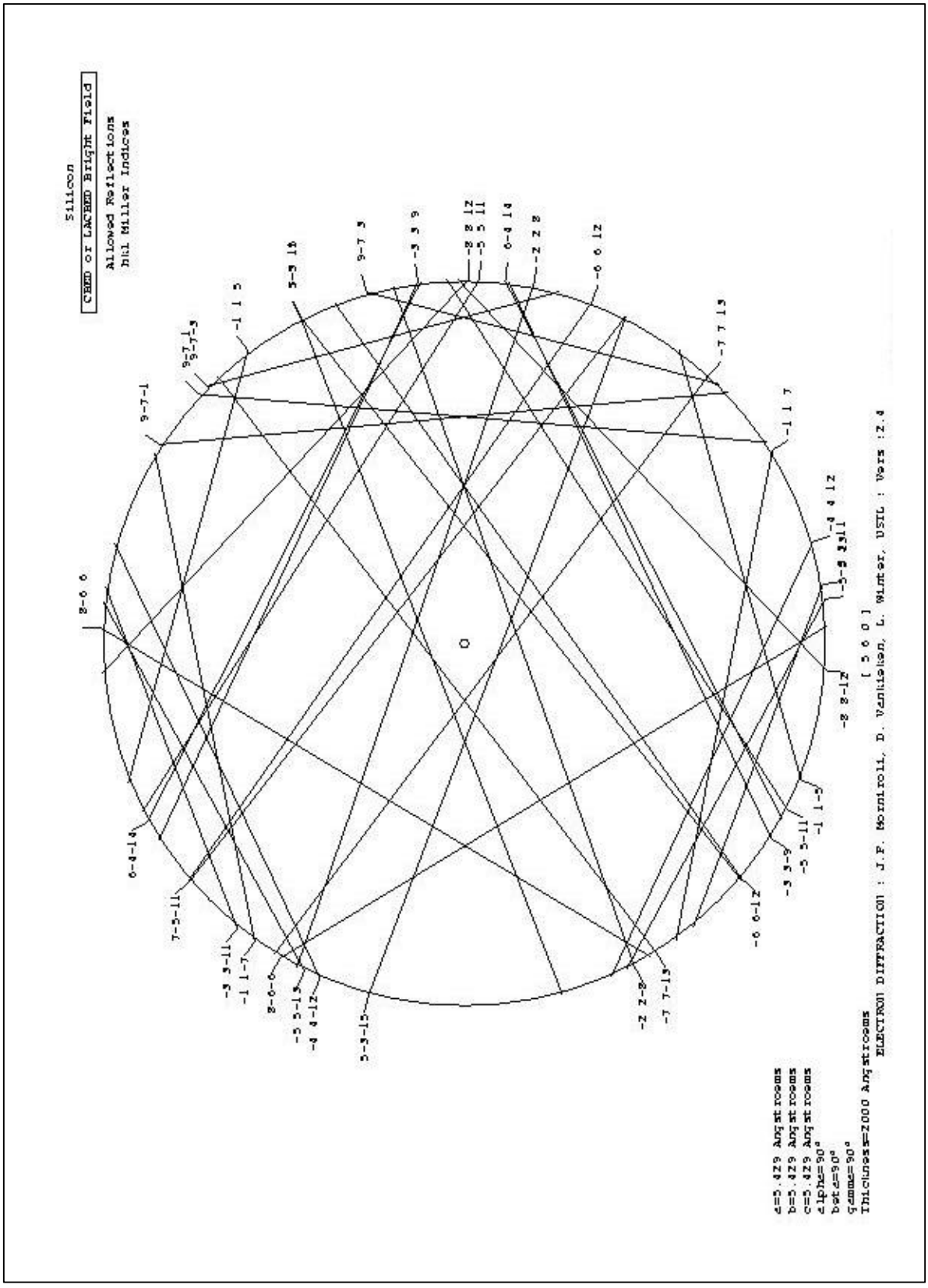

Figure 2.4. a) Simulated CBED pattern taken in the <560> zone axis at 100 kV. The tilt axis, parallel to the <100> growth direction, is horizontal. Tilt angle off the <110> orientation: 5.2°

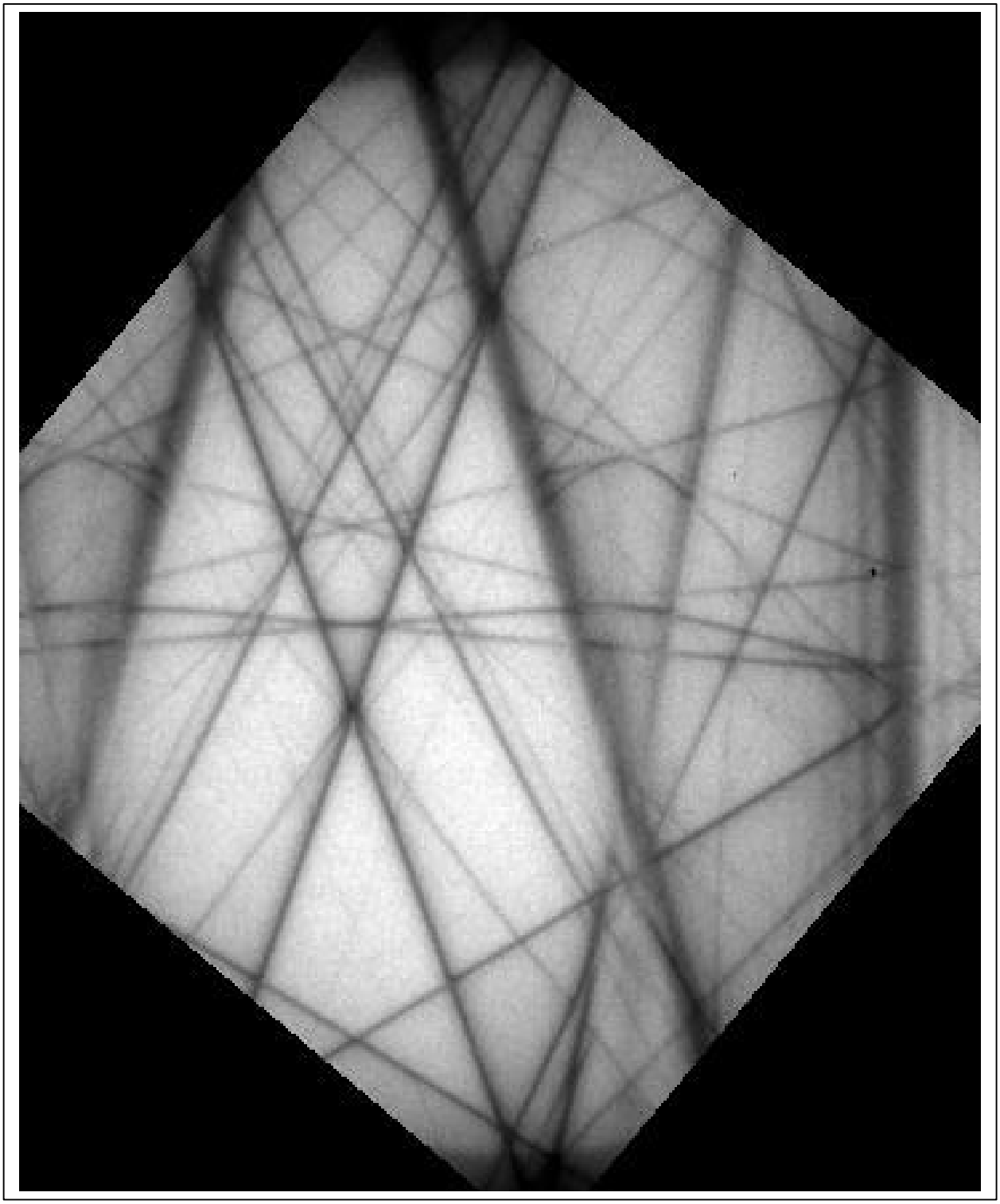

b) Corresponding experimental CBED pattern taken in the <560> zone axis at 100 kV

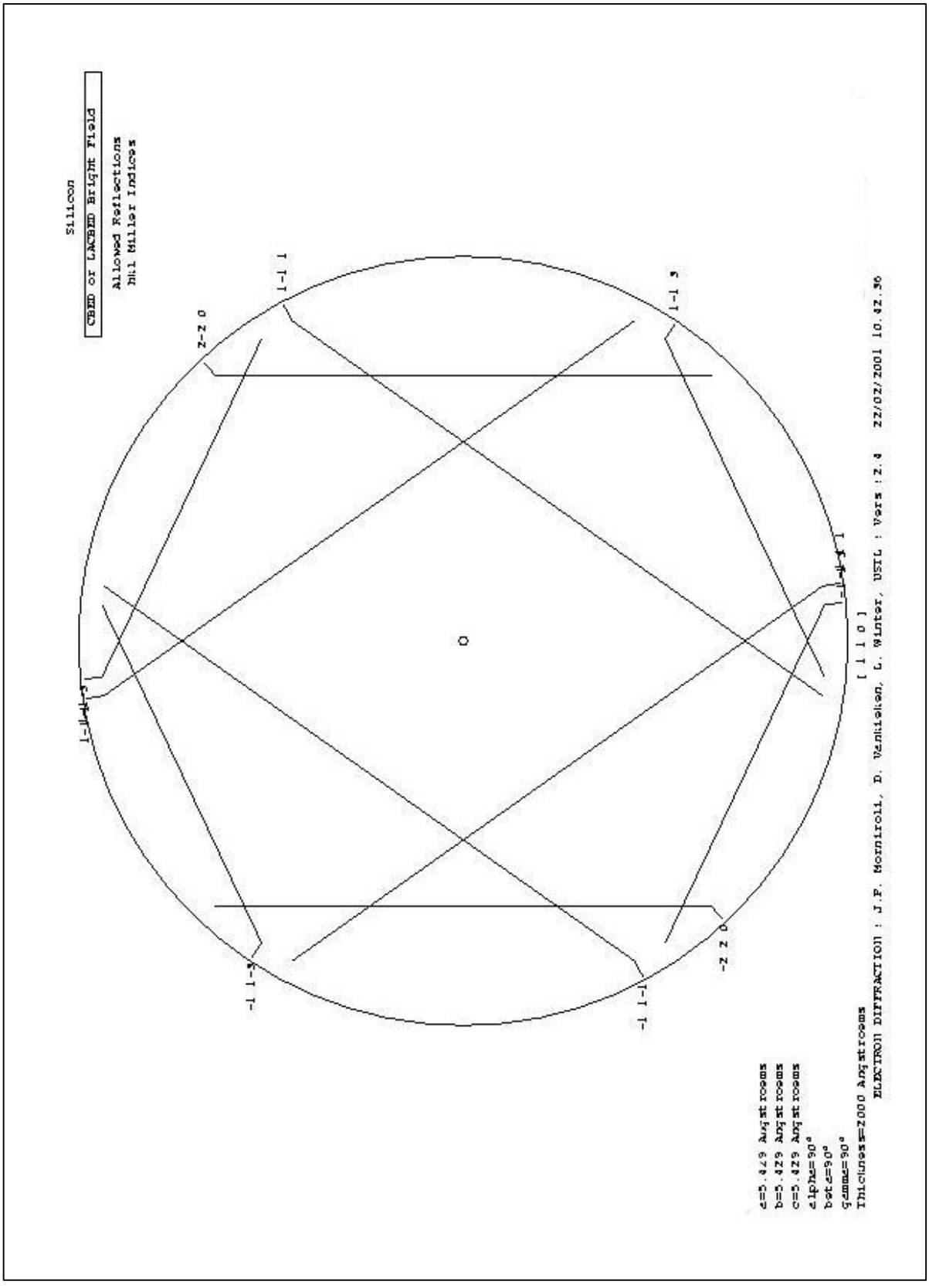

Figure 2.5. a) Simulated CBED pattern taken in the <110> zone axis at 100 kV (no tilt). Note that only lines from the zero order Laue zone (ZOLZ) are present. This is due to the fact that the first HOLZ lines have very large indices and in turn correspond to diffraction planes with very small interplanar spacings; as such, their intensity is very low.

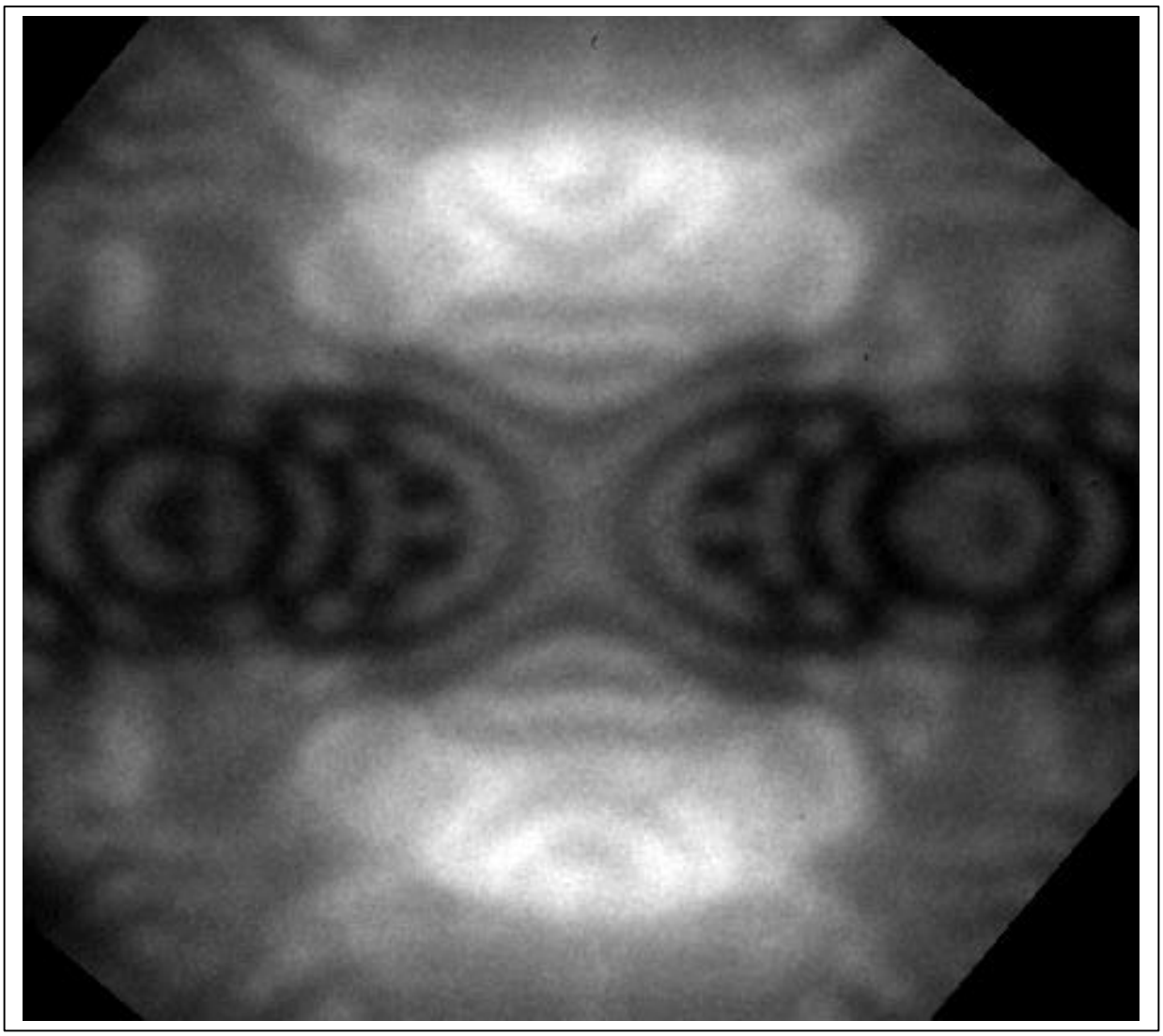

b) Corresponding experimental CBED pattern taken in the <110> zone axis at 100 kV. Note the marked difference with respect to the computed pattern in a). Here only the Bragg contours of the ZOLZ (Zero Order Laue Zone) are visible, the fringe pattern being due to the strong dynamical character of the relevant reflections. Therefore, the kinematical strain analysis in this zone axis is impossible

From the inspection of Figure 2.1 to Figure 2.5 it can be deduced that, apart from the well-known projection <130>:

- The zone axis <120> can be workable, but the reduction in the tilt angle is not that significant, so the axis <230> would be preferred
- The zone axis <560> would be even better (tilt angle of only 5.2°), but the presence of HOLZ lines too close to each other in the pattern renders the skeletonisation of the corresponding experimental pattern difficult
- The zone axis <110> allows the sample to be kept horizontal (no tilt) so it would be of course the first choice. Unfortunately, the absence of HOLZ lines in the CBED pattern prevents this axis from being exploitable.

In summary, the use of the <230> zone axis (tilt angle: 11.3°) can be explored. However, it would be also advisable a parallel increase in the acceleration voltage of the TEM electron beam, thus increasing both the spot intensity and the maximum local thickness of the sample that can be analysed. For this reason, it has not been performed at 100 kV a thorough investigation of a zone axis different from <130>: instead, it has been preferred to carry out the CBED work at 200 kV.

2.2 Simulated and corresponding experimental CBED patterns at 200 kV

The same set of simulations of CBED patterns shown in the previous section, as obtained by the Morniroli [1] programme, have been performed at 200 kV. As before, they refer to the crystal lattice of undeformed silicon.

The simulated patterns for the <230>, <560> and <110> zone axes are reported in Figure 2.8 to Figure 2.10.

It is clearly visible from these figures that CBED patterns taken in the <230> projection at 200 kV contains a reasonable number of HOLZ lines. In fact, the corresponding experimental patterns have proved to be skeletonisable (see Figure 2.7 and also Deliverable D14). It has therefore been decided to carry out a thorough investigation of the capability of CBED analysis to determine strain in the structures of the STREAM project.

The <560> zone axis presents a favourable situation, too. However, the computational work needed to fully exploit a crystallographic projection is very long, consisting of the following steps:

- Choice of a suitable set of HOLZ lines, whose number should be reasonably small (<20); the criteria for this choice is (i) the ease of identification by the software for pattern skeletonisation, which depends on how the line is separated from the adjacent ones; and (ii) the kinematical character of the HOLZ line, which can be assessed through a dynamical simulation
- Choice of the most useful crossing points between couple of HOLZ lines; this step depends on the sensitivity to strain of a given point, which can be ascertained only by running the HOLZFIT programme (now included into the beta-version of the CBED package of AnalySIS) for the maximum possible number of sets of crossing points. A proper strategy must be set up to clearly relate the role of the individual lattice parameters to the shift in the position of each crossing point.
- Modification of the SIS software to allow the user to operate friendly with the new zone axis.

For the time being it has not been undertaken an evaluation activity of the <560> zone axis: it has been preferred to concentrate the efforts on the <230> one, in order to get sufficient information on its adequacy to the strain analysis of the structures of interest for the project.
As it can be seen in Figure 2.6 the projection effect is anyhow markedly reduced by tilting the sample back from the <130> to the <230> projection.

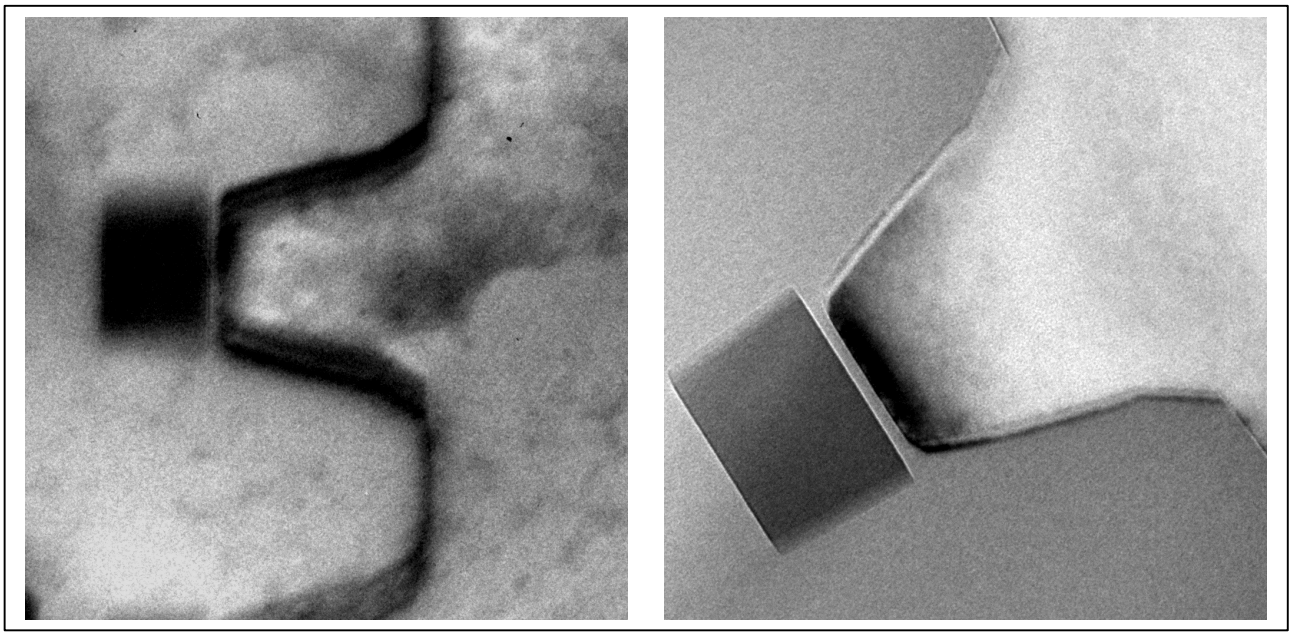

Figure 2.6. Comparison between TEM images taken in the same STI structure of the 1st measurement campaign, but for two different tilt angles. (Left) <130> zone axis at 26.5° off the horizontal <110> projection. (Right) <230> zone axis 11.3° off. Note the remarkable reduction of the projection effect.

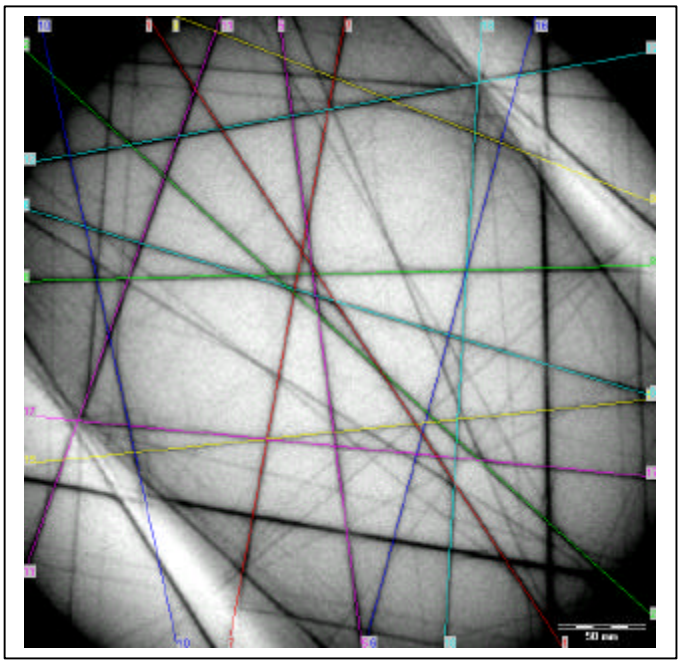

Figure 2.7. Example of skeletonisation of an experimental CBED pattern taken in the <230> projection. Beta-version of the SIS software.

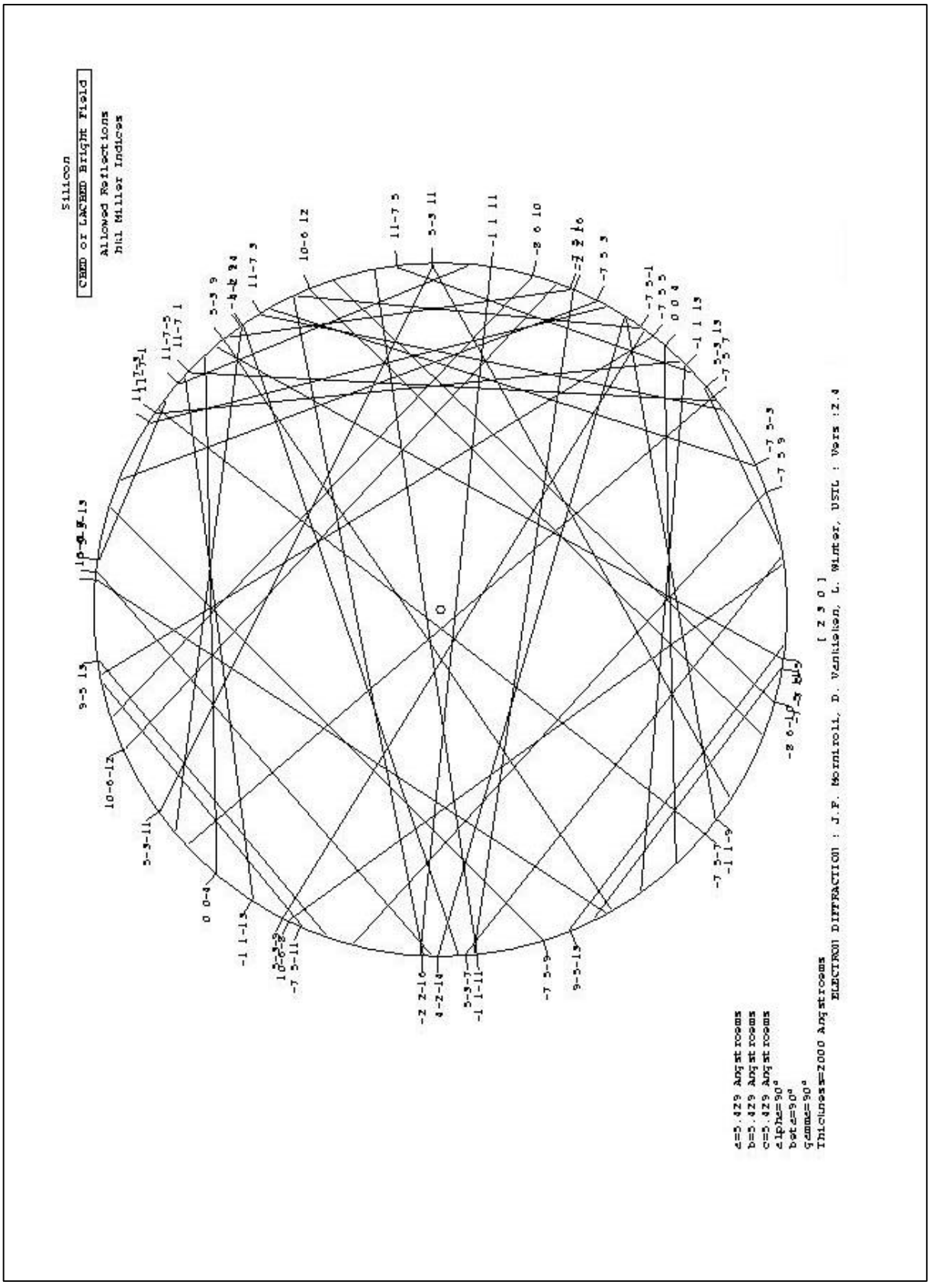

Figure 2.8. a) Simulated CBED pattern taken in the <230> zone axis at 200 kV. The tilt axis, parallel to the <100> growth direction, is horizontal. Tilt angle off the <110> orientation: 11.3°

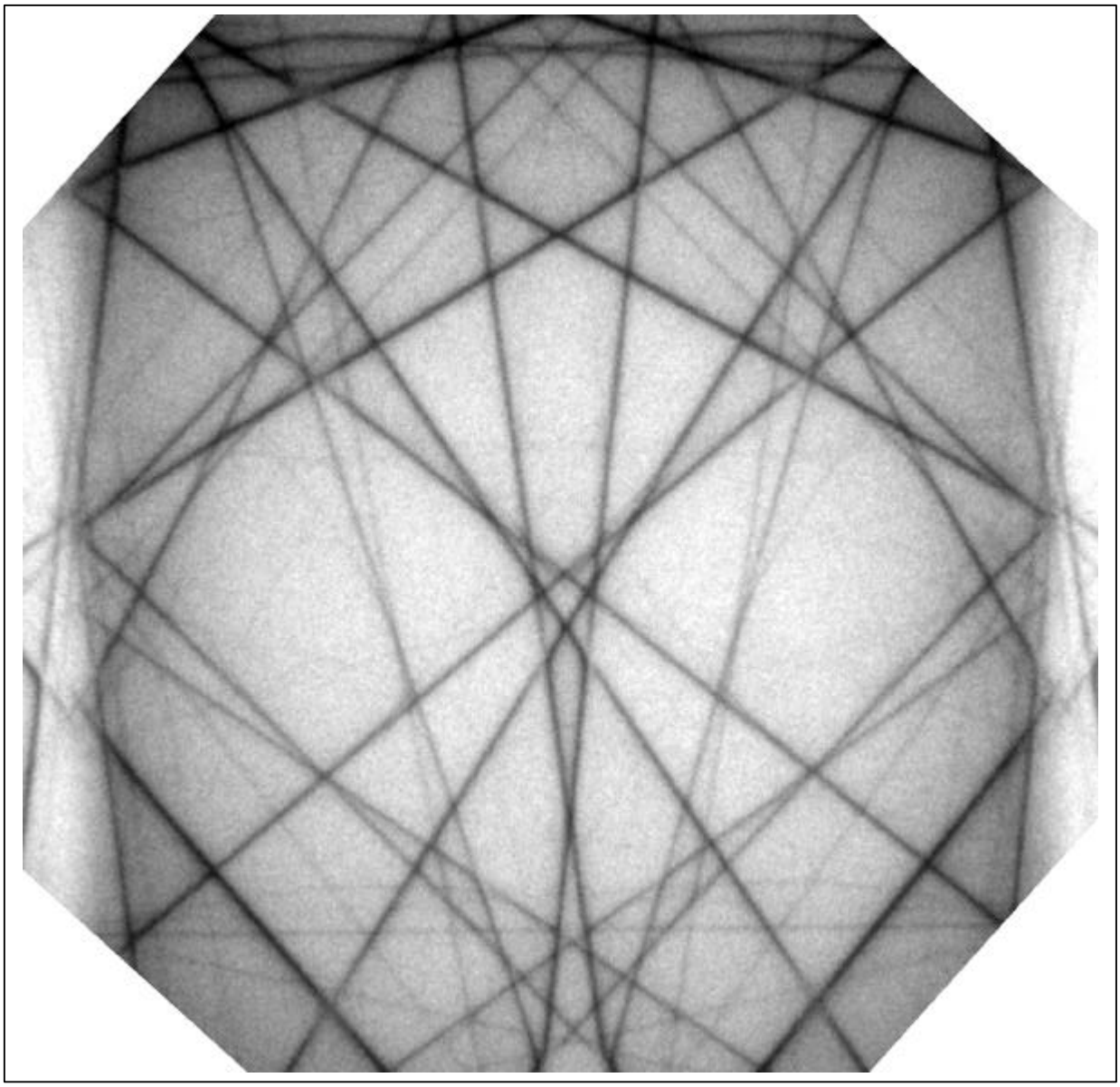

b) Corresponding experimental CBED pattern taken in the <230> zone axis at 200 kV

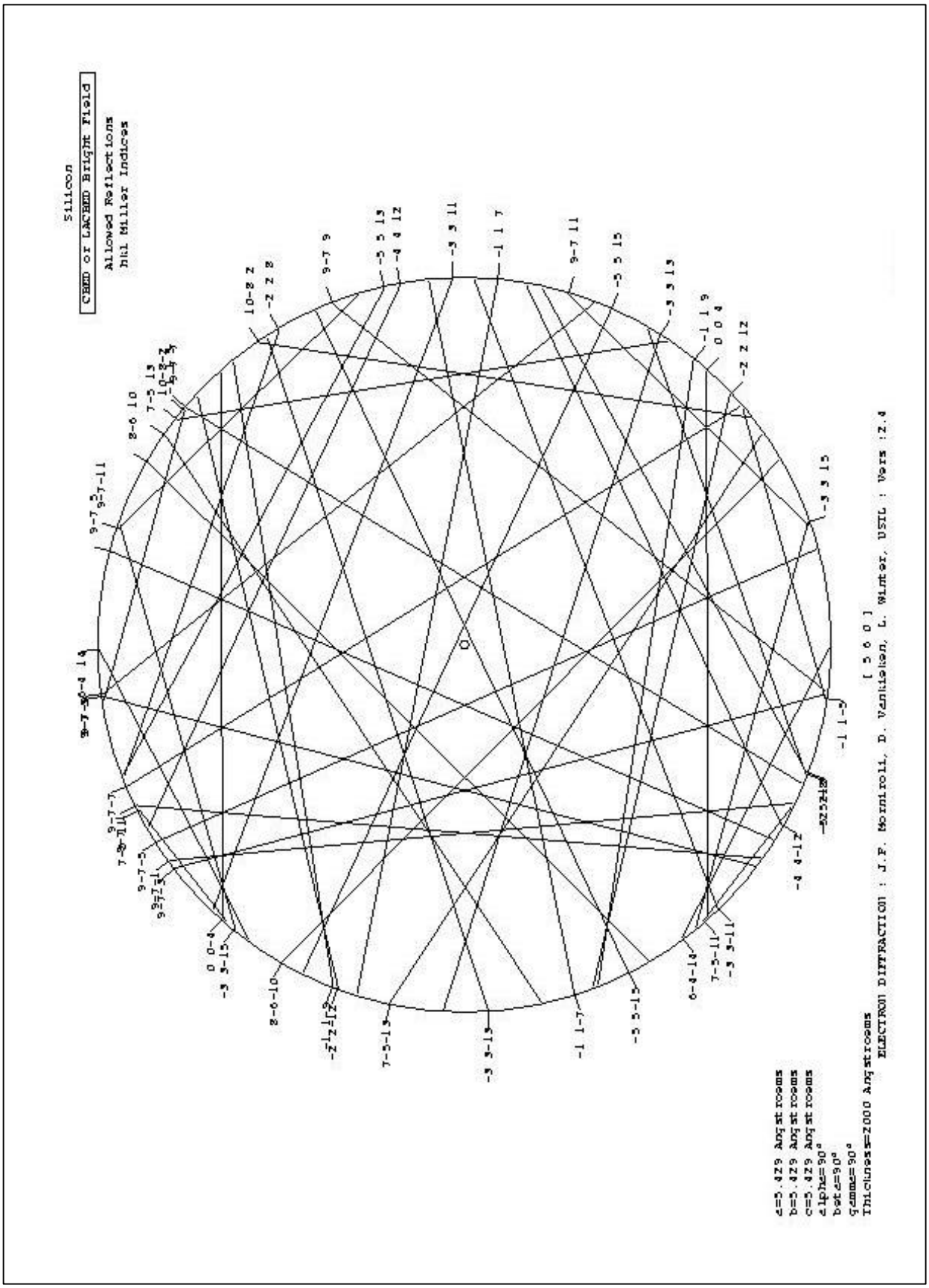

Figure 2.9. a) Simulated CBED pattern taken in the <560> zone axis at 200 kV. The tilt axis, parallel to the <100> growth direction, is horizontal. Tilt angle off the <110> orientation: 5.2°

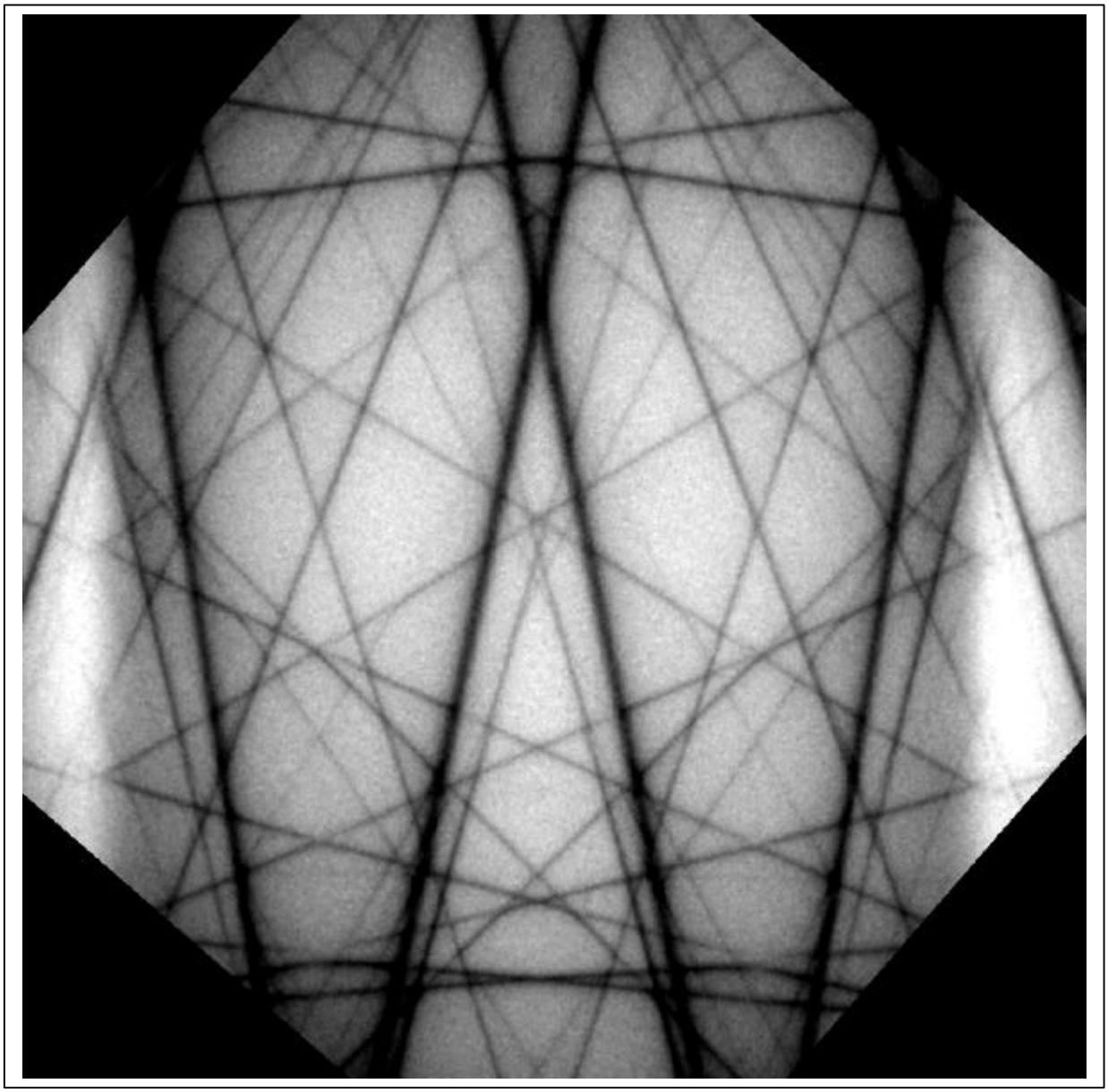

b) Corresponding experimental CBED pattern taken in the <560> zone axis at 200 kV

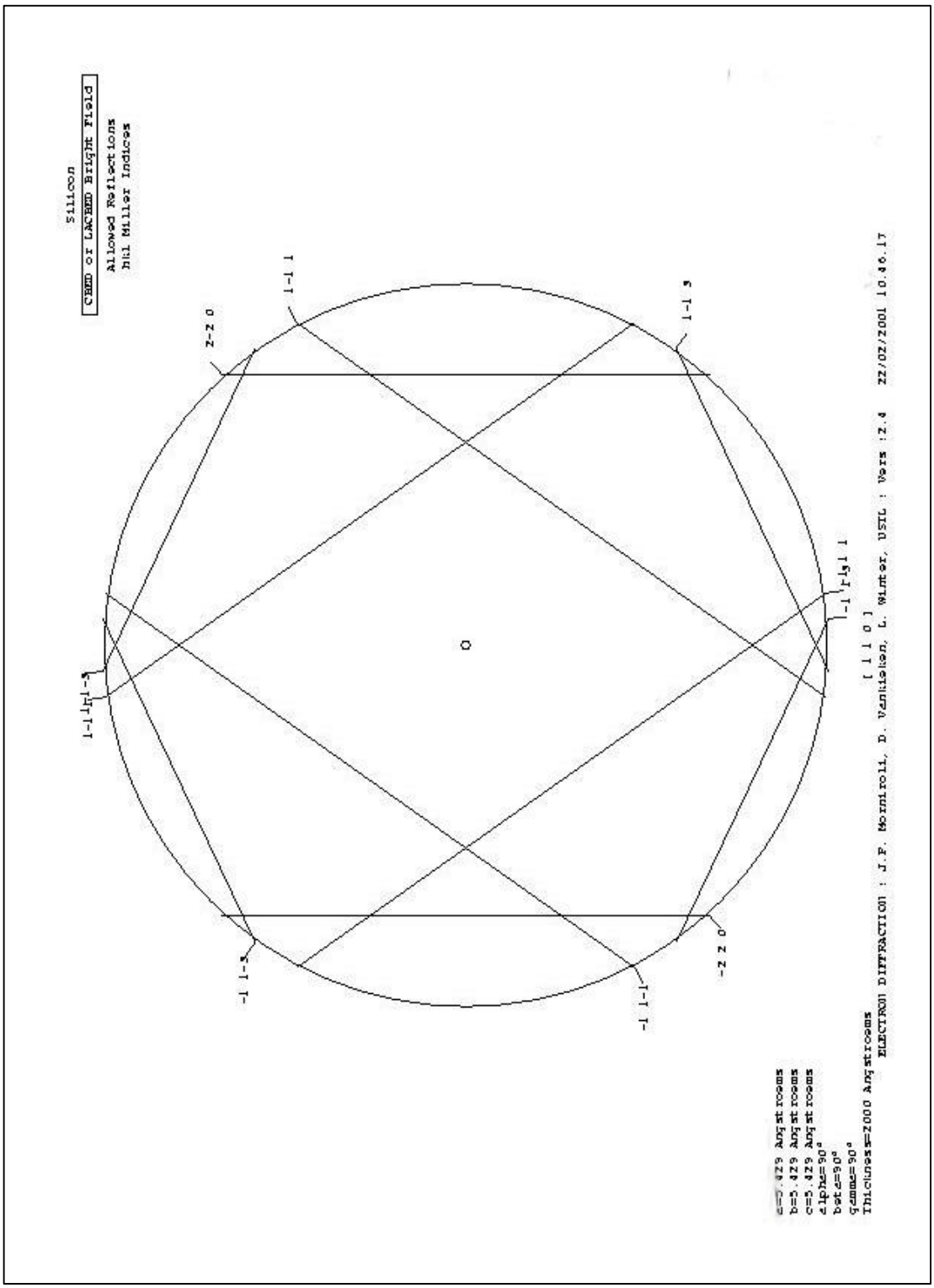

Figure 2.10. a) Simulated CBED pattern taken in the <110> zone axis at 200 kV (no tilt). Like at 100 kV, the pattern consists only of ZOLZ (dynamic) lines, whose arrangement is independent of the acceleration voltage.

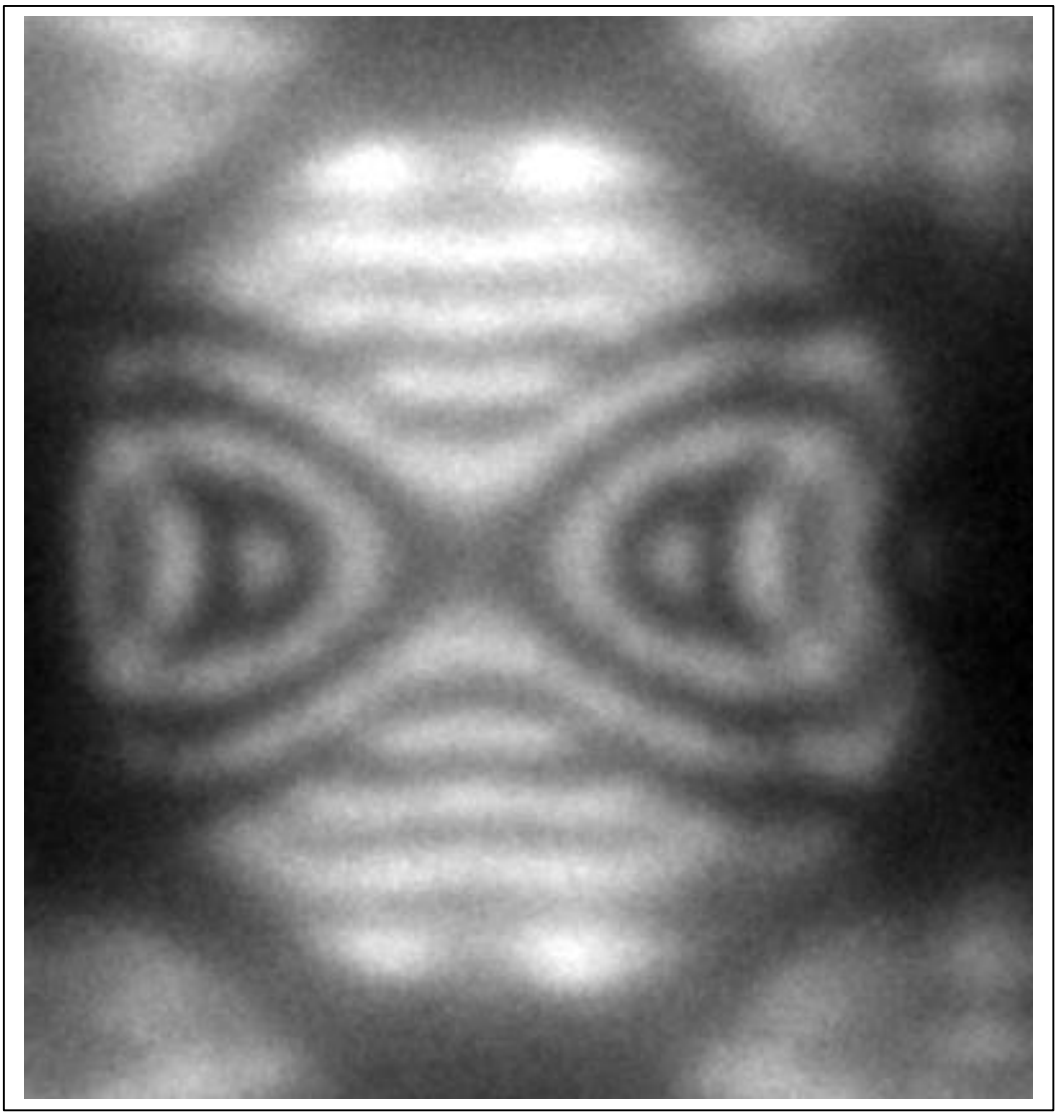

b) Corresponding experimental CBED pattern taken in the <110> zone axis at 200 kV. Note the marked difference with respect to the computed pattern in a). Like in the case of 100 kV (Figure 2.5), only the Bragg contours of the ZOLZ (Zero Order Laue Zone) are visible, the fringe pattern being due to the strong dynamical character of the relevant reflections. It is therefore confirmed that the kinematical strain analysis in this zone axis is impossible

3. Evaluation of the <230> zone axis in the strain analysis by CBED

It is known that the dynamical deviations in a HOLZ line pattern from the corresponding kinematical one are of two kinds: interaction between zero order reflections and HOLZ lines and dynamical interactions between HOLZ lines. The first kind of dynamical effect produce thickness induced shift of HOLZ lines and deviation of the lines from the kinematically expected rectilinear behaviour. The second kind of dynamical effect produces bending of the lines near the point of their intersections. Good results on strain measurements based on fast kinemetical calculations can be then obtained only if the pattern is reasonably free from dynamical effect. In order to study dynamical effects on [230] HOLZ lines pattern we have done the following experiment:
We have first produced dynamical simulation of HOLZ line pattern at 200keV of unstrained silicon at different thickness from 150nm to 240 nm in [230] zone axis. Then we run beta version of SIS software in order to skeletonise the pattern and finally we run HOLZFIT in order to obtain the kinematical fit of the dynamical pattern for different thickness.
We observe the following points:

1. The kinematical best fit is obtained with almost the same effective voltage for all the investigated thickness ±0.03 keV of deviation corresponding to strain indetermination of $6x10^{-5}$); this means that HOLZ lines don't appreciably change their positions with the thickness.
2. The χ^2 value is always less than 1 . This means that the kinematically simulated patterns don't deviates from dynamically ones for more than 1 pixel for each measured distance.

In other words dynamical effects are reasonably small in [230] HOLZ line patterns.
In Figure 3.1 are reported the χ^2 plots showing the behaviour vs thickness and the goodness of the kinematical fit.

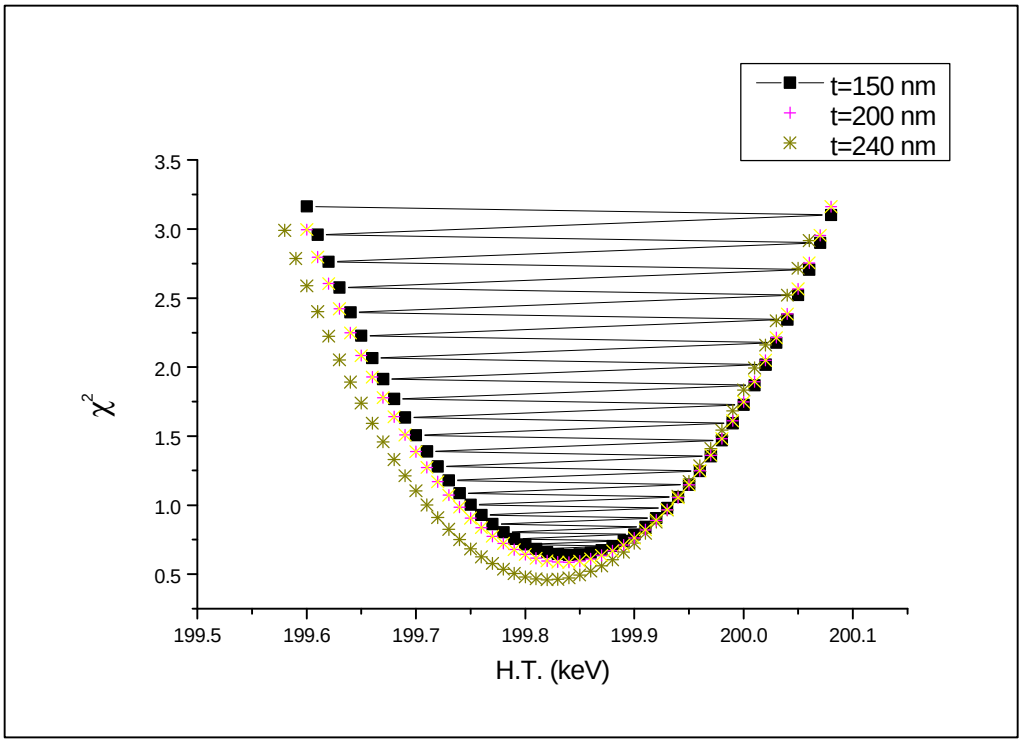

Figure 3.1. Plot of the χ^2-parameter vs. the effective acceleration voltage for different thickness of the sample, as deduced from the kinematical best fit of the dynamical simulation of the corresponding CBED patterns.

The next step in the evaluation of a zone axis is the assessment of the accuracy in the strain determination and the number of components of the strain tensor that can be determined from a single CBED pattern.
To this end, it has been simulated a number of different set of lattice parameters, which correspond to different amounts of strain. This type of calculations is very lengthy, as the crystal symmetry decreases from diamond to triclinic, with a parallel strong increase in the computation time. For this reason, the number of different structures has been limited to 6, yet the results are unambiguous.
In Table 2 are reported the lattice parameters deduced from the analysis, through the beta-version of the SIS software, of the CBED patterns simulated by EMS assuming these six different structures (labelled Strained 1 through 6).

Table 2. Strained silicon lattice cells simulated by EMS and beta-version of SIS software. Δ is the difference between the parameters assumed as an input to EMS and those deduced from the SIS programme.

Structure	**Parameter**	**a (Å)**	**b (Å)**	**c (Å)**	**α (deg)**	**β (deg)**	**γ (deg)**
	Simulated cell	5.425	5.425	5.434	90.02	89.98	89.92
Strained 1	Best fit	5.426	5.426	5.434	90.02	89.98	89.92
	Δ	0.001	0.001	0.	0.	0.	
	Simulated cell	5.424	5.424	5.434	89.98	90.02	89.89
Strained 2	Best fit	5.424	5.424	5.436	89.98	90.02	89.88
	Δ	0.	0.	0.002	0.	0.	0.01
	Simulated cell	5.426	5.426	5.434	89.98	90.02	89.94
Strained 3	Best fit	5.426	5.426	5.436	89.98	90.02	89.93
	Δ	0.	0.	0.002	0.	0.	0.01
	Simulated cell	5.425	5.425	5.433	89.98	90.02	89.92
Strained 4	Best fit	5.425	5.425	5.434	89.98	90.02	89.92
	Δ	0.	0.	0.001	0.	0.	0.
	Simulated cell	5.425	5.425	5.435	89.98	90.02	89.92
Strained 5	Best fit	5.424	5.424	5.436	89.98	90.02	89.91
	Δ	0.	0.	0.001	0.	0.	0.01
	Simulated cell	5.424	5.424	5.435	89.98	90.02	89.89
Strained 6	Best fit	5.424	5.424	5.436	89.98	90.02	89.88
	Δ	0.	0.	0.001	0.	0.	0.01

From Table 2 it comes out that on the accuracy is quite good for all the lattice parameters. On average it is about $1x10^{-3}$ Å ($1x10^{-4}$ nm) for *c* and still better for *a*. The angles α and β are reproduced without errors, that is the sensitivity to shear strain in the (X,Z) and (Y,Z) planes is excellent; this is true also for γ, although the value of this angle is not independent, but related to the diagonal ε_{XX} component of the tensor, according to the plane strain approximation.

It can be concluded that the properties of the <230> zone axes at 200 kV are satisfactory, particularly from the viewpoint of kinematical character and strain sensitivity of the HOLZ lines which appear in the central disk of the corresponding CBED patterns. As such, it can be applied to the strain analysis of the structures of interest to the project. In the next Section it will be reported the results of the application to the samples of the 1st measurement campaign.

4. Strain analysis of the structures of the 1st measurement campaign

In this section it will be reported the results of the strain analysis performed in the structures of the 1st measurement campaign. These structures have been already analysed by TEM/CBED in the 1st semester of the STREAM activity, but in the <130> zone axis and at an acceleration voltage of 100 kV. The results have been presented in the Deliverables D5 and D7. The data reported here refer to the corresponding analyses carried out in the <230> zone axis and at an acceleration voltage of 200 kV, i.e. in the new experimental TEM conditions discussed in the previous sections of this document, that are more favourable than the previous ones. A further difference with respect to the CBED work done before is that the extraction of the strain data from the experimental patterns is now performed by means of the beta-version of the SIS software, whereas in the past the procedure was largely manual.

The strain plots reported in the following refer to CBED analyses performed both at room temperature with energy filtering and at 100 K without filtering. All the structures have a line width of 0.22μm, as reported in Deliverable D5.

4.1 Structures V004808_1_4.

According to Deliverable D1 (and D5) this structure has a nitride thickness of 160 nm, and the oxidation has been done by HDP+TEOS. The strain distribution obtained from CBED patterns taken at 200 kV in <230> axis, along a cutline at z= 100 nm, is reported in Figure 4.1

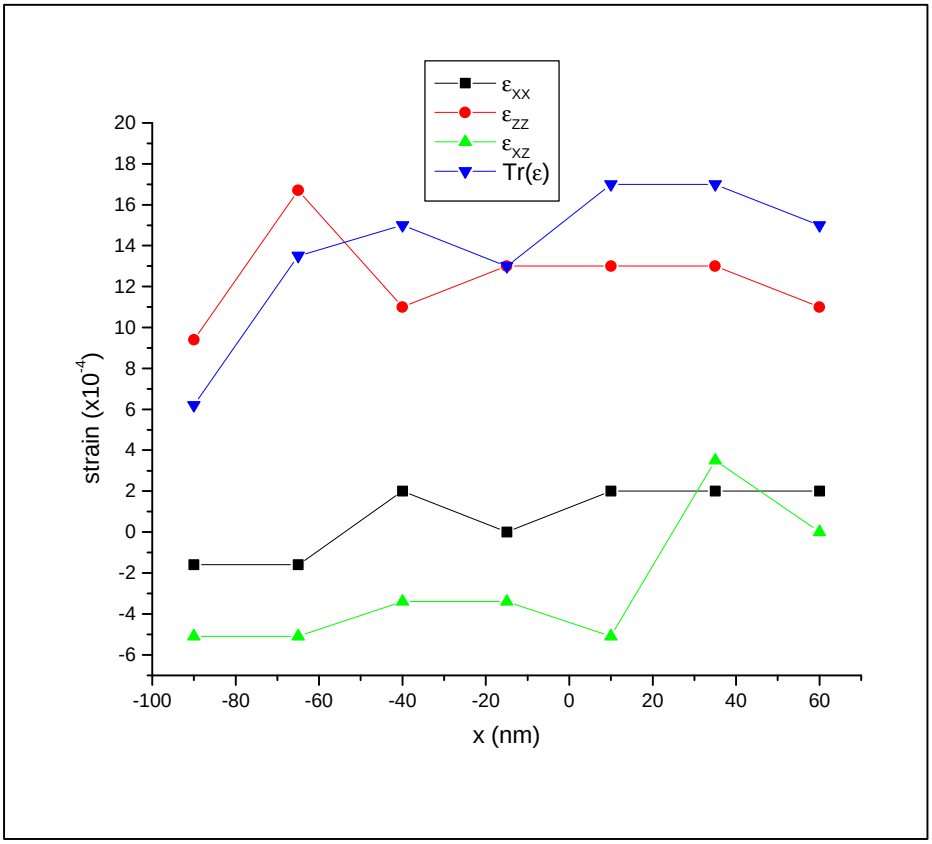

Figure 4.1. Plot of the components of the strain tensor, as well as of the tensor trace; cutline at z=100 nm

4.2 Structures V004808_7_4

In this case the oxidation scheme is based on two HDP steps (HDP1+HDP2), the other parameters are the same as in the previous STI structure. The strain distribution is reported in Figure 4.2

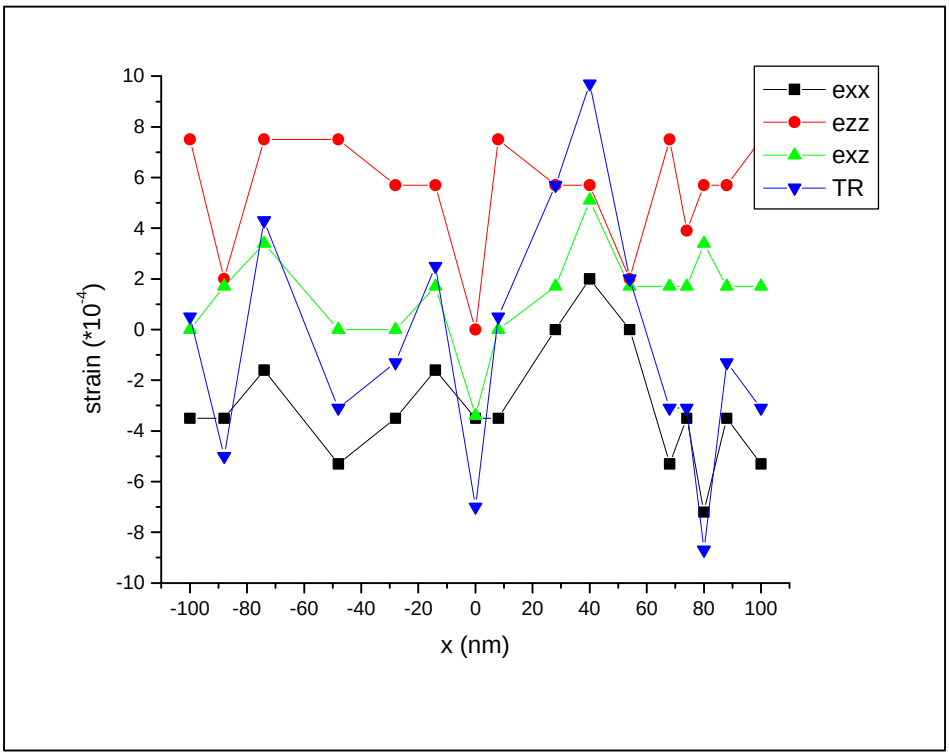

Figure 4.2. Plot of the strain components and of the tensor trace for the structure V004808_7_4. Cutline at z=100 nm.

4.3 Structures V004808_19_4

With respect to the previous 2 structures in this case the thickness of the silicon nitride film is smaller (120 nm instead of 160 nm), whereas the oxidation process is performed with two HDP steps. The corresponding strain distribution at z=100 nm is reported in Figure 4.3

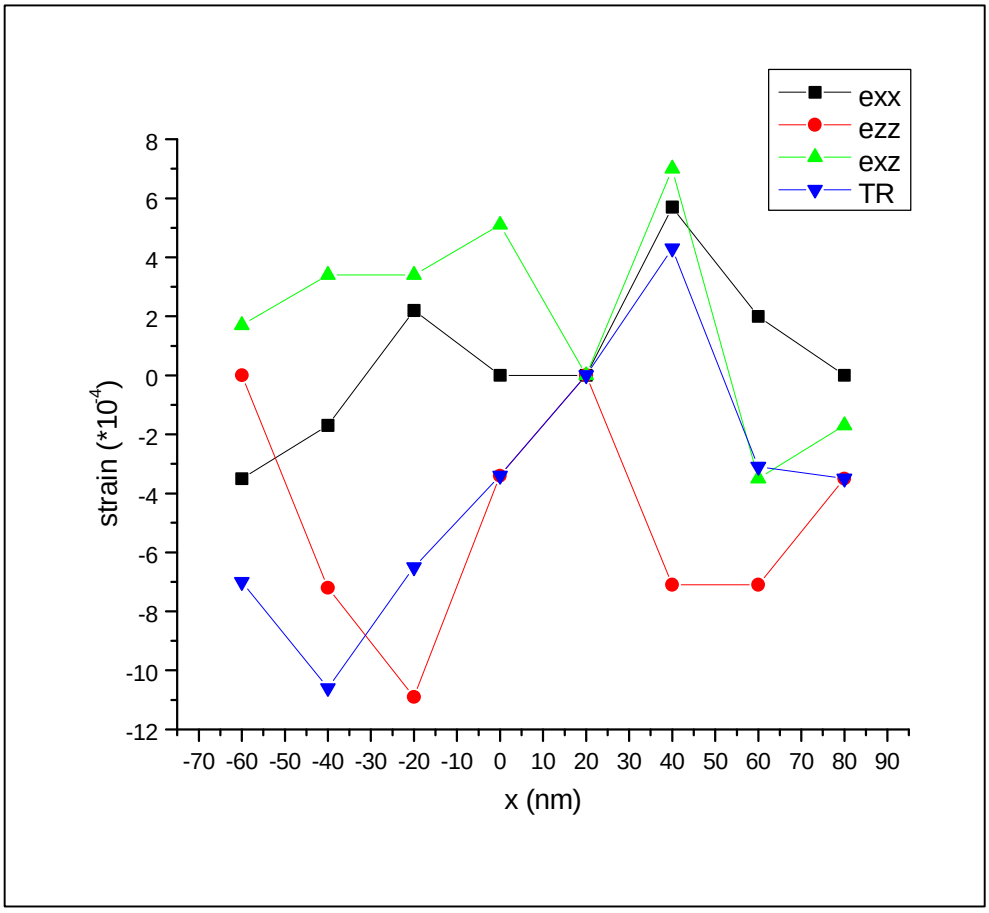

Figure 4.3. Plot of the strain components and of the tensor trace for the structure V004808_19_4. Cutline at z=100 nm.

4.4 Structures V004808_20_4

This structure differs from the previous one only for the densification process, which was absent in all the three STIs previously considered.

The strain distribution for this structure is reported in the next Figure 4.4

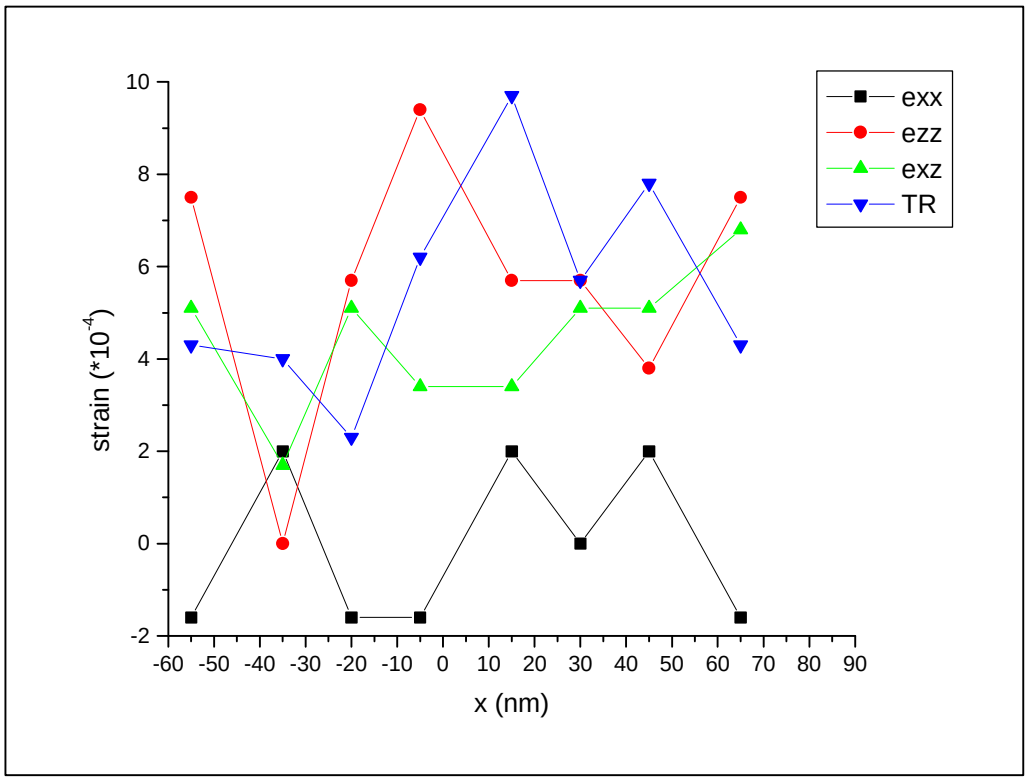

Figure 4.4. Plot of the strain components and of the tensor trace for the structure V004808_20_4. Cutline at z=100 nm.

5. Conclusions

The comparison among the trace of the tensors in Figure 4.1 to Figure 4.4 allows the following conclusions to be drawn:

1. The use of an HDP oxide to get the final thickness, instead of the usual TEOS oxide for trench filling decreases the amount of strain, which is tensile along the cutline. This result, which is deduced by comparing the structure V004808_1_4 (HDP+TEOS) with the structure V004808_7_4 (HDP1+HDP2), is in agreement with the corresponding one found by CBED in <130> zone axis (see Deliv.D7), as well as with the IMPACT calculations (see Deliv. D12a).

2. The decrease in the nitride thickness from 160 to 120 nm does not result in a clear trend, as the trace of the strain tensor oscillates around zero (i.e. shifts from *compressive* to *tensile* along the cutline. The situation was not much clearer in the case of the <130> zone axis (see Deliv. D5).

A slight decrease of the tensor trace in the tensile part of the cutline, however, can be inferred for the case of the thinner nitride.

3. The effect of the oxide densification can be observed by comparing the structures V004808_19_4 and the structure V004808_20_4. For this latter the tensor trace shows a *tensile* behaviour along the cutline. This disagrees with the results found when the CBED patterns were taken in the <130> zone axis. However, it is confirmed that the densification step increases the amount of strain (see Deliv.D5); more precisely, it increases the *tensile* strain at the structure centre, while relaxing the *compressive* behaviour at the edges. This is in agreement with the IMPACT simulations reported in Deliverable D12a.

The difference sometimes observed in the results obtained in the two zone axes (<230> vs. <130>) can be at least in part explained by the different volumes of the sample probed by the TEM electron beam when performing the CBED analysis. Due to the higher tilt angle of the <130> projection off the <110> horizontal one (26.5°), the area explored in the *x* direction is larger than in the <230> one. Therefore, regions with different amount of strain can be explored in the two cases. Moreover, as mentioned above, thicker active areas of the STI structures can be investigated at the higher acceleration voltage employed for the <230> CBED experiments.

6. References

[1] J.P.Morniroli, D.Vankrieken and L.Winter Electron Diffraction, Vers: 2.4 (University of Lille, 1995)